Journal of Photochemistry and Photobiology A: Chemistry 219 (2011) 101–108

Contents lists available at ScienceDirect

Journal of Photochemistry and Photobiology A: Chemistry

journal homepage: www.elsevier.com/locate/jphotochem

Water disinfection using photosensitizers supported on silica

A.K. Benabbou[a,b], C. Guillard[b], S. Pigeot-Rémy[b], C. Cantau[c], T. Pigot[c], P. Lejeune[d], Z. Derriche[a], S. Lacombe[c,*]

[a] Laboratoire Physico-Chimie des Matériaux Catalyse et environnement LPCM-CE, Université des Sciences et de la Technologie d'Oran – BP 1505, El M'naouer, Oran, Algeria
[b] Institut de Recherche sur la Catalyse et l'Environnement de Lyon (IRCELYON), UMR5256, CNRS-Univ. Lyon 1, 2 Avenue Albert Einstein, 69626 Villeurbanne Cedex, France
[c] UMR CNRS 5254, IPREM (Institut Pluridisciplinaire de Recherche sur l'Environnement et les Matériaux), Université de Pau et des pays de l'Adour, Hélioparc, 2 Avenue Pdt Angot, 64053, Pau Cedex 09, France
[d] Microbiologie Adaptation et Pathogénie, Univ. Lyon 1, UMR 5240, MAP – Bâtiment André Lwoff, 43 Boulevard du 11 novembre 1918, 69622 Villeurbanne Cedex, France

ARTICLE INFO

Article history:
Received 24 September 2010
Received in revised form 26 January 2011
Accepted 27 January 2011
Available online 3 February 2011

Keywords:
Photocatalysis
Supported Photosensitizers
Microorganisms inactivation
Water disinfection
Singlet oxygen
Photodynamic inactivation (PDI)

ABSTRACT

The disinfection efficiency against *Escherichia coli* in water of new silica-based materials containing aromatic photosensitizers (APS) was compared to that of TiO_2 under UV irradiation. The APS used in these experiments (9,10-anthraquinone-4-carboxylic acid (ANT) and a recently investigated cyanoaromatic, 9,14-dicyanobenzo[b]triphenylene-3-carboxylic acid (DBTP-COOH)) were grafted onto commercial silica materials. The influence of several physical and chemical parameters on the photoinduced inactivation of the microorganisms was considered: amount of catalysts, APS structure and concentration in the host material.

While no bacterial inactivation took place in the presence of silica in the dark and in the absence of silica under UVA, a slow bactericidal effect was observed in the presence of pure silica under UVA. ANT and DBTP based-materials improved the bacterial inactivation rate under UVA irradiation. The Chick and Watson analysis of the results (without taking into account the induction period observed with all the silica materials), at the same material concentration allowed to conclude that the bacterial inactivation rate constant, k, is the highest ($0.13\,L\,g^{-1}\,min^{-1}$) for SiO_2–ANT with an anthraquinone concentration of $280\,\mu mol\,g^{-1}$ and no longer increased with ANT concentration. This catalyst was more efficient than $SiNH_2$–DBTP ($k = 0.02\,L\,g^{-1}\,min^{-1}$). The latency period for bacterial inactivation with the APS based materials was longer than that observed with TiO_2/UVA, but when using 0.25 g of materials, SiO_2–ANT had a k ($0.720\,L\,g^{-1}\,min^{-1}$) three times higher than TiO_2 ($0.256\,L\,g^{-1}\,min^{-1}$). If the actual photosensitizer or TiO_2 *molar concentration* were examined, it was concluded that all the k values determined for the sensitizer containing silica are much higher (from 305 to $4717\,L\,mol^{-1}\,min^{-1}$) than that obtained for TiO_2 ($24.5\,L\,mol^{-1}\,min^{-1}$). This result emphasizes the high catalytic efficiency of the silica materials containing low amounts of aromatic PSs.

The influence of adsorption of the materials on the microorganisms was shown and the results discussed according to the possible Reactive Oxygen Species. Different mechanisms were proposed for TiO_2 and for the supported sensitizers.

1. Introduction

Supplying drinkable and clean water, free of chemical and biological pollutants, represents an actual technological challenge, especially in the least developed regions of the globe. Besides the widespread chlorination treatment, alternative disinfection methods must be considered for water sterilization [1]. Disinfection processes such as boiling water and Solar Disinfection (SODIS) were successfully used to inactivate various disease-causing microorganisms [2]. Nevertheless, theses technologies showed some weaknesses like:

- Limited water volume subject to treatment.
- Need of combustible material for boiling water [3].
- Long process time to achieve complete inactivation, particularly in SODIS method [4].

Water sterilization by ozonisation was also used as a chemical disinfection process. Although highly efficient against microorganisms, this method leads to the formation of several disinfection by-products such as aldehydes, ketones and carboxylic acids [5]. Advanced oxidation technologies are most often used for

* Corresponding author.
E-mail address: sylvie.lacombe@univ-pau.fr (S. Lacombe).

1010-6030/$ – see front matter © 2011 Elsevier B.V. All rights reserved.
doi:10.1016/j.jphotochem.2011.01.023

microorganisms elimination. For instance, the heterogeneous photocatalytic process has been considered for water disinfection. This technology is based on the interaction of light (UVA) with semi-conductor particles (most often titanium dioxide) to produce highly Reactive Oxygen Species (ROS) which not only destroy bacteria but also oxidize organic and inorganic matters in water [6,7]. Moreover, the production of significant amounts of hydrogen peroxide by illuminated TiO_2 was shown to inactivate bacteria and to ensure a disinfection durability by inhibiting *E. coli* regrowth [8]. Several parameters influencing the TiO_2 mediated photocatalytic disinfection were studied. The effect of TiO_2 concentration, light intensity, dissolved salt concentration, pH and spectral range (UVA, UVB, UVC) were discussed in many papers [9–11]. However, the UVA dependence may limit the use of titanium dioxide as photocatalyst under solar activation. To circumvent this difficulty, photosensitized oxidation reactions based on photochemically active compounds in catalytic amounts (Aromatic Photosensitisers or APS), may be considered [2,3]. The elimination of microorganisms using APS is known as antimicrobial Photo-Dynamic Inactivation (PDI) [12], and it uses visible light to activate the photosensitizers. APS were also used in Photo-Dynamic Therapy (PDT), efficient for the destruction of cancer cells under visible light [13]. The absorption of a photon by a photosensitizer leads to the production of ROS according to two pathways:

(i) Radicals formation, issued from electron transfer from the photosensitizer to molecules in its direct environment (Type I photo-oxidation reaction). In the presence of air, the most often produced ROS is thus superoxide radical-anion, $O_2^{\bullet -}$.
(ii) Energy transfer from the triplet excited state of photosensitizers to the ground state of oxygen, generating singlet oxygen, $^1O_2$ (Type II photo-oxidation reaction).

Both pathways can lead to cell death [14]. $^1O_2$ would be particularly damageable for every type of cells from prokaryotic to mammalian, which could undergo an irreversible damage leading to their death [15–19]. Implication of PDI in water treatment is still under research. Bonnett et al. tested several photosensitizers in *E. coli* inactivation and demonstrated that the chitosan/phthalocyanine association was the most effective to inactivate microorganisms [20]. Also, Gram negative, Gram positive bacteria and fungi had been efficiently inactivated by a single cationic photosensitizer, e.g., 5-phenyl-10,15,20-tris(N-methyl-4-pyridyl)porphyrin (TriP[4]) [21–23] or toluidine blue [24–26]. Most of PDI procedures employed photosensitizers molecules mixed to bacterial suspensions in homogenous aqueous media [21–32]. Accordingly, it is difficult to recover the dissolved photosensitizers from water once the treatment finished. Recent papers by Manjón et al. demonstrated the efficiency of Ru(II) coordination complexes immobilized on porous silicone for water disinfection in solar reactors [2,3]. In the present paper, two silica-supported photosensitizers were tested against bacteria inactivation. Silica is transparent to irradiation, even if silica particles strongly scatter UV light. The materials were commercial silica powders or beads, on which the photosensitizers were introduced by covalent grafting. These materials were tested as powders suspensions on *E. coli* inactivation using UVA and visible light, the long-term aim being to develop a PDI procedure totally based on solar inactivation. The results of PDI are compared with those obtained by TiO_2 photocatalysis disinfection.

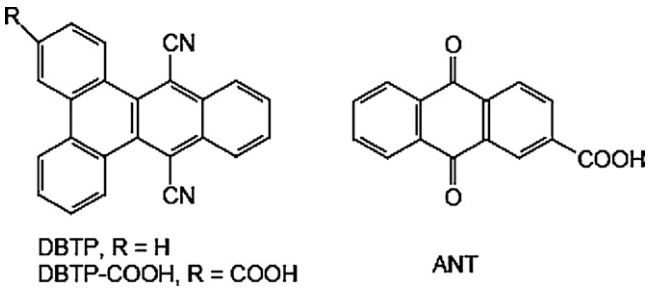

Scheme 1.

2. Materials and methods

2.1. Preparation of photosensitizers

The detailed description of the synthesis and characterization of most of these silica materials were already published [33]. Two APS (Scheme 1), were tested in the present work:

- A carboxylic derivative of benzo-[b]triphenylene-9,14-dicarbonitrile (DBTP): 9,14-dicyanobenzo[b]triphenylene-3-carboxylic acid (DBTP-COOH) recently described.
- 9,10-Anthraquinone 2-carboxylic acid or ANT.

DBTP-COOH is a recently developed cyanoaromatic, with a characteristic absorption band between 400 and 420 nm, patented as an efficient APS [34]. On the other hand, ANT was already used for different photo-oxidation reactions, both in organic solutions [35] and at the gas–solid interface [36]. Both APS may be efficiently activated at 420 nm.

APS grafting onto silica was made according to two different procedures [33]:

- ANT was converted to its triethoxysilyl derivative by condensation with (3-aminopropyl) triethoxysilane (APTES) and grafted to commercial silica beads (Acros, 3–5 mm diameter, pore diameter *ca.* 9 nm, surface area 400 $m^2\,g^{-1}$), by reflux in toluene and washing in several solvents. The corresponding material is named SiO_2–ANT in the following.
- DBTP-COOH was also grafted on a commercial amino-functionalized silica powder ($SiNH_2$, Aldrich, 40–63 μm particles, 1 mmol g^{-1} NH_2, surface area 550 $m^2\,g^{-1}$) under reflux in toluene and washed with various solvents. The corresponding material is called $SiNH_2$–DBTP in the following.

The disinfection efficiency of the previously described materials was compared with the bactericidal effect of titanium dioxide (TiO_2 Degussa P25, 80% anatase, 20% rutile, density 3.8 g cm^{-3}, average particle size 20–30 nm, surface area 50 $m^2\,g^{-1}$), introduced in a disinfection process in a previous work [11]. The beads SiO_2–ANT or the reference material (SiO_2 beads) were finely grinded in a mortar and sieved through a 80 μm mesh. $SiNH_2$–DBTP was used as prepared.

2.2. Characterization of the prepared materials

The synthesized photosensitizers were characterized using Diffuse Reflectance UV spectroscopy (DRUV) on a Varian Cary 5E apparatus equipped with an integrating sphere. Conventional UV spectroscopy in solution was also used to determine the amount of non-grafted APS in the reflux solution after grafting, thus giving an estimate of grafted APS on silica [33].

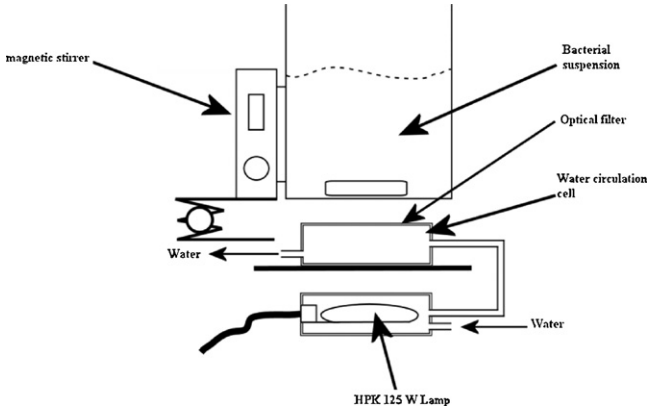

Scheme 2. Irradiation device.

The surface area of the materials and their pore size were evaluated through nitrogen adsorption and desorption isotherms of the silica xerogels, measured at 77 K on a Micromeritics ASAP 2010 Micropore nitrogen adsorption apparatus.

2.3. Disinfection and photochemical experiments

The disinfection experiments were carried out in a 90 mL pyrex reactor, with 20 mL of solution (water pH 6–7). To ensure complete mixing, the materials/*E. coli* slurry was magnetically stirred. Three sets of disinfection experiments were carried out, varying the following parameters: (1) nature of the photosensitizer, (2) weight of the photosensitizing material and (3) concentration of the photosensitizer in the material. The effect of pure powdered silica (host material containing no APS) on the microorganisms was also studied. To conclude, the inactivation efficiencies of titanium dioxide and of the photosensitizing materials were compared under the same conditions.

The disinfection experiments were carried out at room temperature, using air as oxidant.

The photosensitizing materials (or pure silica) were introduced at two different concentrations (0.25 and 2.5 g L^{-1}). A Phillips HPK 125 W lamp, emitting in the 200–600 nm range, was used as UV light source. The "0.52" Corning filter was used to cut off any radiation below 340 nm (UVA). The irradiation device is depicted in Scheme 2. Lamp emission spectrum and filters transmission spectra are given in supplementary information (SI).

Light intensities were measured with a VLX-3W radiometer, equipped with 365, 312, and 254 nm captors for monitoring UVA irradiation at 365 nm. To measure the intensity, captors were put at various distances from the light source. For the disinfection experiments, the reactor containing the bacterial suspension to be disinfected was maintained at a distance of 3 cm from the water circulation cell. Values of lamp intensities in UVA and visible domains are listed in Table 1. The disinfection experiments were repeated three times to check the reproducibility of the results.

For the photo-oxidation experiments, the reacting mixtures (10^{-2} M di-*n*-butylsulfide in acetonitrile containing 2.6×10^{-3} M and 1.6×10^{-4} M ANT and DBTP, respectively, in order to achieve a solution absorbance of $A = 1$) were continuously bubbled with oxygen through a mass flow-meter (2 cm^3 mn^{-1}) during the irradiation. The reactor was placed inside a RAYONET® device containing four RAYONET fluorescent lamps with maximum emission at 420 nm and irradiated for 150 min. At the end of irradiation, product analysis was performed by GC (VARIAN 3900 with a FID detector, l5 m CP-Sil-5 Chrompack column, i.d.: 0.25 mm, coating 0.25 μm) or by GC–MS (HP 5973, SPB35 column, *l*: 60 m, i.d.: 0.23 mm). Acidic products were extracted by adding to 1 cm^3 of the CH_3CN oxidized solution, 2 cm^3 of water and 2 cm^3 of dichloromethane. Acid titrations of the aqueous phase were performed by Ion Exchange Chromatography (IEC) on a Dionex DX-20 Exchange Ion Chromatophraph equipped with a column AS9-HC (4 mm) operating in the suppressed conductivity mode.

Table 1
Irradiance of the lamp at 365 nm and in the visible range.

Height (cm)	1	2	3
Intensities (mW cm^{-2}), UVA (λ = 365 nm)	7	5.1	3.9

2.4. Analysis and culture of bacteria

The bacterial strain used in this work was PHL1273, a derivative of the *E. coli* K-12 strain MG1655. It was constructed by G. Jubelin (unpublished) by transformation of the strain PHL818 [37] using the plasmid pPHL127. PHL 818 carries the chromosomal mutation omp R234 which results in the overproduction of curli, a particular type of fimbriae allowing the bacteria to adhere to abiotic surfaces [38]. pPHL127 is a derivative of the pPROBE-gfp[LVA] (stratagene) containing the csgBA promoter in front of the gfp[LVA] reporter gene. No differences in terms of cell wall constitution (outer and inner membranes) of *E. coli* PHL1273 were noticed by comparison of the original strain (MG1655). Due to its curli overproduction, PHL1273 can stick to surfaces and form biofilms. It was used as biological pollutant in previous works [11,44] *E. coli* bacteria was inoculated into Luria Bertani medium [39], mixed with water 1/1, and grown overnight at 30 °C, with constant agitation, under aerobic conditions. Bacterial growth was monitored by measuring the optical density at 600 nm. At a stationary growth phase, bacteria were harvested by centrifugation in a 1.5 mL Eppendorf tube at 10^3 rounds per min during 3 min, and washed twice with 1.5 mL of water. An *E. coli* stock suspension was prepared by resuspending the final pellets in 1.5 mL of water. The initial populations of *E. coli* ranging, approximately, from 10^5 to 10^6 cfu mL^{-1} (colony forming unit) were obtained by diluting the stock suspension. The cell concentrations were determined by the spread plate method, with nutrient agar grown at 37 °C during 18 h. The volume of 0.1 mL of suspension was withdrawn at each sampling and was diluted to 1/10, 1/100, and 1/1000. Some of the samples were spread without diluting. Finally, 100 μL of the diluted and undiluted suspensions were spread to count the number of *E. coli*. Three replicate plates were used at each dilution.

2.5. The Chick–Watson modelisation

The Chick–Watson kinetic model ($\ln N/N_0 = -kCt$) was used in order to compare the results obtained under the different experimental conditions. In this model, N_0 represents the initial *E. coli* population (cfu mL^{-1}), N the remaining *E. coli* population at time t (cfu mL^{-1}), C the disinfecting material concentration (mg L^{-1}), k the inactivation rate constant (L min^{-1} g^{-1}) and t the inactivation time (min). This model was applied to our experimental data considering C as the catalyst concentration used for the inactivation process. The induction period in the inactivation curves and the tail of the curves were not taken into account for the model application. A complementary calculation was carried out with the photosensitizer *molar concentration* (in L min^{-1} μmol $^{-1}$) to compare the effective activated photosensitizer *molar concentration* to that of TiO_2.

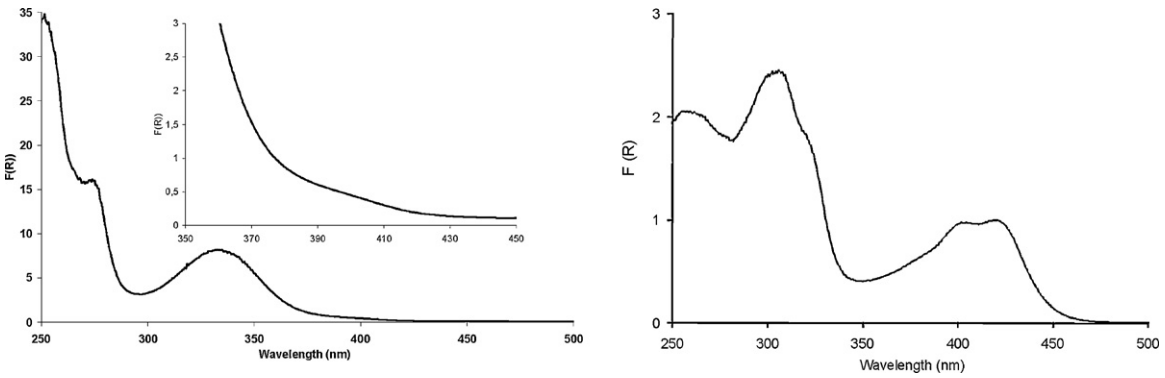

Fig. 1. DRUV spectra of (left) SiO_2–ANT and (right) $SiNH_2$–DBTP.

3. Results and discussion

3.1. Photosensitizers characterization

Table 2 summarizes the values of the aromatic photosensitizers concentrations in hosts materials, as well as the specific area and the porosity of the synthesized materials.

The concentration of DBTP-COOH after grafting on the $SiNH_2$ material was 27 μmol g^{-1}. A higher ANT concentration was achieved on non-amino functionalized commercial silica beads (280 μmol g^{-1}). For this material the specific area varied from 400 m^2 g^{-1} before grafting to 280 m^2 g^{-1} after grafting of ANT. The DRUV spectra of the materials are given in Fig. 1. The spectrum of SiO_2–ANT (Fig. 1, left) was characteristic of anthraquinone, with a very low-intensity n–π* transition between 380 and 430 nm [36]. The spectrum of $SiNH_2$–DBTP (Fig. 1, right) showed an intense absorption band between 340 and 450 nm with vibration components characteristic of anthracene derivatives [33].

3.2. Disinfection test in the presence of pure silica with irradiation at λ > 340 nm

It was first necessary to test the behaviour of the host material alone (grinded commercial silica beads without any photosensitizers, particles size < 80 μm) towards microorganisms, and the corresponding *E. coli* inactivation curves are presented in Fig. 2.

A bacterial inactivation was observed in the presence of pure silica irradiated with λ > 340 nm. Curves A and B in Fig. 2 show the reproducibility of the bacterial inactivation test under these conditions: the bacterial population decreased from 10^6 to 10^7 cfu mL^{-1} to less than 10^2 cfu mL^{-1} after 360 min of irradiation. No bacterial inactivation was noticed either in the presence of silica in the dark or by photolysis (irradiation of the suspension without any added material). The following assumptions can be proposed to account for this result:

(i) The silica aggregates could stick and concentrate around microorganisms, making them more vulnerable to the UVA irradiations in these scattering suspensions, and the contact between silica particles and *E. coli* surface could induce a stress to the microorganisms making them less resistant against external attacks. Light scattering by silica materials not only depends on the particles size, but also on their shape, morphology, surface heterogeneity and refractive index and could vary on the spectral wavelength range. Complementary study should be necessary to determine the influence of the light scattering coefficient of pure silica, among other parameters, on its bactericidal activity.

(ii) It is accepted that UVA and UVB may cause cellular damage in the presence of oxygen, mainly due to light absorption by intracellular chromophores and main formation of superoxide radical-anion [40]. To the best of our knowledge, no similar result was found in the literature dealing with the effect of pure silica on microorganisms under irradiation, although it is known that mesoporous silica nanoparticles inhibited respiration of isolated mitochondria and submitochondrial particles [41]. Further studies showed that cytotoxicity appears to be related to the adsorbtive surface area of the particle, although the nature of functional groups on silica cannot be ruled out [42].

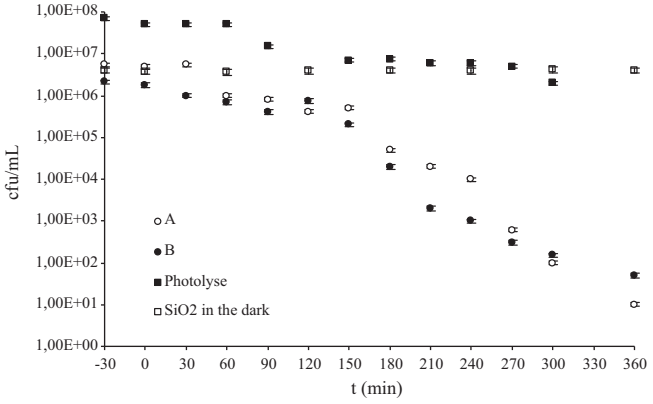

Fig. 2. *E. coli* irradiation in the presence of pure silica (2.5 g L^{-1}) in the dark and under λ > 340 nm irradiation (365 nm intensity: 3.9 mW cm^{-2}). A and B correspond to two runs for identical experiments with pure silica, photolysis corresponds to a similar experiment without any added silica. The period between −30 and 0 min corresponds to the adsorption step in the dark.

Table 2
Materials characterization: mode of synthesis, APS nature and concentration, specific surface area and porosity.

Material name	Elaboration of the silica matrix (APS–silica interaction)	APS	[APS] (μmol g^{-1})	Specific surface area (m^2 g^{-1})	Porosity
$SiNH_2$–DBTP	Commercial SiO_2–NH_2 post-grafting	DBTP-COOH	27	650	Mesoporous
SiO_2–ANT	Commercial SiO_2 post-grafting	ANT	280	280	Mesoporous

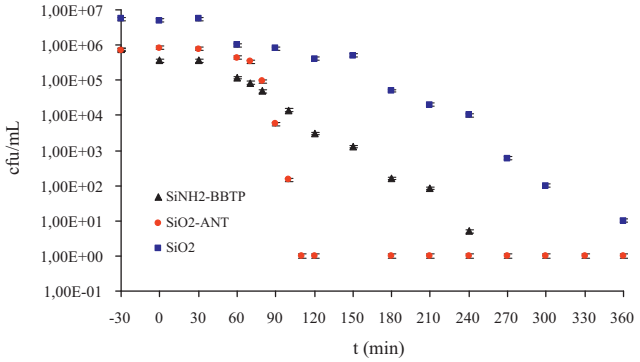

Fig. 3. *E. coli* inactivation in presence of 2.5 g L^{-1} various supported photosensitizers under irradiation with $\lambda > 340$ nm (365 nm intensity 3.85 mW cm^{-2}). The period between −30 and 0 min corresponds to the adsorption step in the dark.

3.3. *E. coli* inactivation using photosensitizers and irradiation at $\lambda > 340$ nm

The inactivation efficiency of the supported photosensitizers was evaluated by introducing the materials in the bacterial suspensions irradiated with UVA. Fig. 3 shows *E. coli* inactivation in presence of the considered photosensitizers. In all cases, a long induction period before bacterial inactivation was observed. The shortest induction period was about 30 min using $SiNH_2$–DBTP. SiO_2–ANT gave a slightly longer induction period, but became more effective once the *E. coli* inactivation began. *E. coli* concentration decreased to an undetectable level after 110 min of UVA irradiation with this latter material and after 240 min with $SiNH_2$–DBTP. The long induction period constitutes the main difference relative to TiO_2 (see below), as established in a previous work [11,43,44]. Efficiencies of the photosensitizers involved in water disinfection are summarized in Table 3.

A much slower *E. coli* inactivation was observed in presence of anthraquinone and DBTP-COOH based materials under visible light ($\lambda > 428$ nm). The inactivation rate under these conditions was comparable to that observed with pure silica. It can thus be considered that no APS activation took place under filtered visible light (Fig. S2). These results were not surprising since the absorption bands of ANT and DBTP were very weak at $\lambda > 428$ nm (Fig. 1) and the light source used in this study poorly emits between 420 and 450 nm (Fig. S1).

These results are to be compared with other chemical experiments made with similar materials [45]. First, it was previously shown that DBTP (R = H, Scheme 1) or anthraquinone embedded in highly transparent silica monoliths, prepared by the sol–gel method and exhibiting the same absorbance at 350 nm were able to produce singlet oxygen under UVA irradiation in air (*i.e.* without any solvent). The singlet oxygen quantum yield relative to phenalenone in the same materials, measured at the gas–solid interface by time-resolved luminescence of singlet oxygen at 1270 nm, were, respectively, 0.89 ± 0.04 and 0.8 ± 0.1 for DBTP and ANT containing silica monoliths. Singlet oxygen lifetime in these air-equilibrated monoliths was determined around 30 μs.

Table 3
Data of *E. coli* photocatalytic inactivation, using various photosensitizing materials.

Material name	Induction period (min)	Total inactivation time (min)	Remaining [*E. coli*] (cfu mL^{-1})
$SiNH_2$–DBTP	30	240	5
SiO_2–ANT	60	110	0
Commercial SiO_2	90	Non-achieved (360 min)	50

Table 4
Product distribution of di-*n*-butylsulfide (DBS) photooxidation experiments in homogeneous solution in acetonitrile (DBSO = di-*n*-butylsulfoxide, $DBSO_2$ = di-*n*-butylsulfone, DBDS = di-*n*-butyldisulfide, acidic compounds = *n*-butanesulfonic and sulphuric acids).

PSA/product	DBS	DBSO	DBSO2	DBDS	Acidic compounds
DBTP	<1	94	4	1	<1
ANT	13	53	2	12	20

Second, di-*n*-butylsulfide photooxidation experiments (with fluorescent lamps with maximum emission at 420 nm) in homogeneous solution in acetonitrile were carried out with DBTP and ANT. In both cases, efficient oxidation to mixtures of di-*n*-butylsulfoxide (DBSO) and di-*n*-butylsulfone ($DBSO_2$) was observed, with various amounts of di-*n*-butyldisulfide (DBDS), *n*-butyl-*n*-butanethiosulfonate ($DBSSO_2$) and acidic compounds, indicative of C–S bond cleavage (Table 4). It was previously shown [35], that DBDS, $DBSSO_2$ and acids, arising from radical mechanisms after C–S bond cleavage, were related to electron-transfer (Type I) mechanism and possible formation of superoxide radical anion. In the present case, from the analysis of the reaction products, it was concluded that singlet oxygen was mainly involved with DBTP, while electron transfer reaction was also possible with ANT, leading to larger amounts of DBDS, $DBSSO_2$ and several acidic compounds. Even if the life time of singlet oxygen is very dependent on the solvent (3–7 μs in water and *ca.* 60 μs in acetonitrile), these results in homogeneous acetonitrile solution support the conclusion on singlet oxygen production by $SiNH_2$–DBTP and of singlet oxygen and superoxide anion with SiO_2–ANT.

From these results, several conclusions may be drawn on the efficiency of the materials under investigation:

(1) For the newly developed photosensitizer, DBTP-COOH, it may be inferred that the APS concentration in the material, as well as its mode of incorporation on silica, plays a crucial role. Actually, two other DBTP based materials were used for the photo-bactericidal tests. These materials prepared according to a sol–gel method with inclusion of APS in much lower concentration and probably located inside the silica walls, were totally inefficient for water disinfection. The only efficient DBTP based material was also the most loaded, $SiNH_2$–DBTP (27 μmol g^{-1}). Moreover, when grafting DBTP-COOH on commercial amino-functionalized silica, it may be assumed that DBTP is located on surface amino-functions inside the pores of the materials, and thus closer to the microorganisms. Hence, the generated ROS, especially $^1O_2$, could diffuse more easily to the microorganisms and inactivate them.

(2) SiO_2–ANT beads, heavily loaded with anthraquinone derivative (280 μmol g^{-1}), was the most efficient material. Although the quantum yield of singlet oxygen production by anthraquinone embedded in silica xerogel was previously found slightly lower (0.8 ± 0.1) than that of DBTP (0.89 ± 0.04) relative to phenalenone in the same medium [45], this result confirms previous observations on the high photo-oxidation efficiency of ANT [36]. It may tentatively be related to the fact that anthraquinone is susceptible to sensitize photo-induded oxidation reactions by either type II (with singlet oxygen $^1O_2$ production) or type-I mechanism (electron transfer and radical production, including superoxide radical-anion, $O_2^{\bullet -}$). In water, $O_2^{\bullet -}$ is able to react as a strong Bronsted base via formation of HOO• and hydrogenperoxide, two species known as powerful bactericidal reactants [46].

(3) Adsorption of the materials on the microorganisms is probably necessary. The lifetime of singlet oxygen, $^1O_2$, which is only 3–7 μs in water, makes it possible to cross only very short

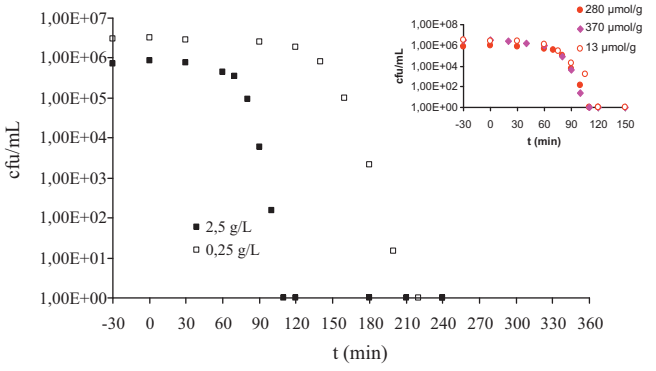

Fig. 4. Effect of the amount of SiO_2–ANT in aqueous suspension on the bacterial inactivation ([ANT] = 2.8×10^{-4} mol g^{-1}) under irradiation at $\lambda > 340$ nm. Insert: Influence of the anthraquinone concentration in the material in a suspension containing 2.5 g L^{-1} of SiO_2–ANT ([ANT] = 280, 374 and 13 µmol g^{-1}). The period between −30 and 0 min corresponds to the adsorption step in the dark.

distances not exceeding 0.1 µm [47]. Thus, the microorganisms must take time to diffuse towards silica particles, to closely link to the material in order to allow the generated $^1O_2$ to reach targets on *E. coli*. A previous comparison of the efficiency of supported or non-supported photosensitizers showed that the bacterial inactivation was faster in homogeneous medium [31] than in heterogeneous one [3].

3.4. Effect of material amount and of ANT concentration on the bacterial inactivation by SiO_2–ANT

SiO_2–ANT was the only photosensitizer material that achieved a total *E. coli* elimination within 110 min under UVA irradiation. Its bactericidal property against *E. coli* was tested at two concentrations: 0.25 and 2.5 g L^{-1}. The initial populations of *E. coli* ranged approximately from 10^5 to 10^6 cfu mL^{-1}. Curves of *E. coli* inactivation with two materials amounts are given in Fig. 4. The corresponding Chick and Watson analysis of the whole set of experiments is summarized in Table 5.

The reduction by ten times of the material amount led to a significant increase of the total inactivation time (from 110 to 220 min), correlated with an increase of the induction period. The Chick–Watson slope decreased from 0.32 to 0.18 min^{-1}, even if the rate constant of bacterial inactivation increased significantly (from 0.13 to 0.72 L g^{-1} min^{-1}) when going from 2.5 g to 0.25 g L^{-1} of material, evidencing the efficiency even at low silica amounts. This result could tentatively be assigned to the drop of singlet oxygen (or any other ROS) production, related to the decrease of the APS (ROS generator) amount. On the contrary, it is worth recalling that under similar conditions, the increase of TiO_2 amount in the suspension induced a screening effect, resulting in a drop in efficiency of bacterial elimination for the high TiO_2 concentrations [11].

However, the insert of Fig. 4 shows that a variation of the anthraquinone concentration in the material (between 13 and 374 µmol g^{-1}) had only a slight effect on the microorganisms inactivation rate: *E. coli* was inactivated using 2.5 g L^{-1} of any of the three materials containing various amounts of anthraquinone. The induction period did not change and the determined inactivation slopes varied from 0.32 to 0.15 min^{-1} on decreasing ANT concentration (Table 5). By comparing the experiment with 0.25 g L^{-1} of SiO_2–ANT ([ANT] = 280 µmol g^{-1}, *i.e.* 70 µmol L^{-1} of ANT in the suspension) and the one with 2.5 g L^{-1} of SiO_2–ANT ([ANT] = 13 µmol g^{-1}, *i.e.* 32.5 µmol L^{-1} of ANT in the suspension) in Table 5, the Chick–Watson slopes were of the same order of magnitude (0.18 and 0.15 min^{-1}, respectively) while the ANT

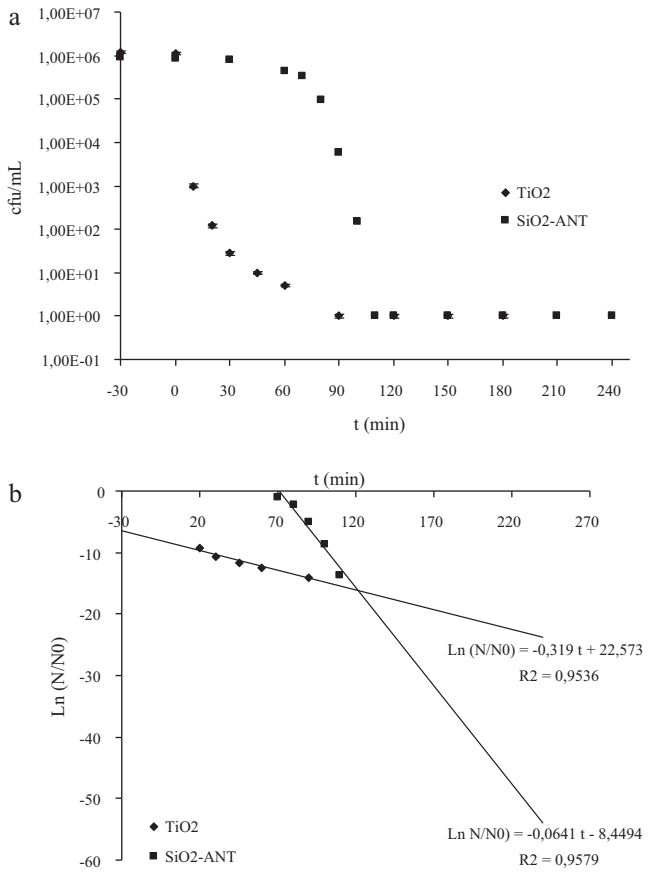

Fig. 5. (a) Photocatalytic inactivation of *E. coli* in presence of 0.25 g L^{-1} of TiO_2 or 2.5 g L^{-1} of SiO_2–ANT under UVA light ($\lambda > 340$ nm). The period between −30 and 0 min corresponds to the adsorption step in the dark; (b) Chick–Watson curve of *E. coli* inactivation kinetics in presence of TiO_2 or SiO_2–ANT.

concentration increased by a factor 2. Accordingly, the efficiency of the materials is not only related to the amount of available anthraquinone, as assumed above when comparing the mass of the two materials introduced in the suspension (Fig. 4). The surface of the material also plays a crucial role, as the catalyst need to get linked or adsorbed onto bacteria in order to allow the *E. coli*–sensitizer interaction. With lesser amount of material, it can be assumed that all the available silica is adsorbed on the bacteria for an efficient bactericidal effect, which is probably not the case when using larger amounts of material.

3.5. Comparison between TiO_2 efficiency and photosensitizing materials

The photocatalytic inactivation efficiency using TiO_2 or photosensitizing materials as catalysts was used for comparison. Actually, the comparison for *E. coli* inactivation was carried out using the most efficient SiO_2–ANT material. Fig. 5a and b gives, respectively, the bacterial inactivation curves in the presence of the two materials at their optimum concentrations *i.e.*: 2.5 g L^{-1} for SiO_2–ANT (280 µmol g^{-1}) and 0.25 g L^{-1} for TiO_2 and the Chick–Watson modelisation for bacterial inactivation kinetics with TiO_2 and SiO_2–ANT. Materials were activated by UVA and the initial bacterial population was about 10^6 cfu mL^{-1}.

The main difference between the two photocatalysts was the induction time: while TiO_2 action onto microorganisms was immediate, SiO_2–ANT showed a latency period of 60 min as described previously. However with both catalysts, total inactivation was reached after 90 min of UVA irradiation. Once activated, SiO_2–ANT

Table 5
Determination of the Chick and Watson slopes according to the mass of materials and to the molar concentration of the photosensitizers/photocatalysts. *k* are the rate constant of bactericidal inactivation related either to the mass of materials ($L\,g^{-1}\,min^{-1}$) or to their molar concentration ($L\,mol^{-1}\,min^{-1}$).

	SiO_2	SiO_2–ANT (M_{ANT} = 252 g mol^{-1})				$SiNH_2$–DBTP (M_{DBTP} = 372 g mol^{-1})	TiO_2
		13 μmol g^{-1}	280 μmol g^{-1}	374 μmol g^{-1}	280 μmol g^{-1}		
g L^{-1}	2.5	2.5	2.5	2.5	0.25	2.5	0.25
μmol L^{-1}	–	32.5	700	935	70	67,5	3125
Chick and Watson slope (min^{-1})	0.03 ± 0.01	0.15 ± 0.04	0.32 ± 0.06	0.29 ± 0.06	0.18 ± 0.04	0.06 ± 0.01	0.06 ± 0.01
k (L g^{-1} min^{-1})	0.010 ± 0.002	0.06 ± 0.01	0.13 ± 0.02	0.11 ± 0.02	0.72 ± 0.008	0.020 ± 0.002	0.26 ± 0.04
k (L mol^{-1} min^{-1})		4717 ± 200	456 ± 50	305 ± 50	2570 ± 100	807 ± 100	24.5 ± 10

needed only 30 min to decrease the bacteria population to a non-detectable level, and the slope (Table 5) is in this case much steeper (0.32 min^{-1}) than with TiO_2 (0.06 min^{-1}).

From the analysis of the whole set of Table 5 data, it may be concluded that pure silica gives the slowest inactivation slope (0.03 min^{-1}), and that the slopes determined for $SiNH_2$–DBTP and TiO_2 were of the same order of magnitude (0.06 min^{-1}). The steepest slopes were obtained with SiO_2–ANT (from 0.15 to 0.32 min^{-1}) depending on the material mass and ANT concentration.

Comparison of the results at the same material concentration allowed the following conclusions on the bacterial inactivation rate constants:

- For SiO_2–ANT, *k* was maximum for an anthraquinone concentration of 280 μmol g^{-1} (0.13 L g^{-1} min^{-1}) and no longer increased with ANT concentration.
- The *k* determined for SiO_2–ANT (0.13 L g^{-1} min^{-1}) was higher than for $SiNH_2$–DBTP (0.02 L g^{-1} min^{-1}).
- *k* value, with 0.25 g L^{-1} of SiO_2–ANT material (0.720 L g^{-1} min^{-1}), was three times higher than that for TiO_2 (0.256 L g^{-1} min^{-1}). However it must be recalled that a long induction period was noticed for SiO_2–ANT.
- When taking into account the molar concentration of active species (Table 5, last line), all the *k* values determined for the sensitizer containing silicas were much higher (from 305 to 4717 L mol^{-1} min^{-1}) than that obtained for pure TiO_2 (24.5 L mol^{-1} min^{-1}), as the molar concentration of the active PS on silica is much lower (up to two order of magnitude) than the molar concentration of TiO_2. This result emphasizes the high catalytic efficiency of the silica materials containing low amounts of aromatic PSs.

Some differences made the comparison between the two kinds of catalysts difficult:

- 2.5 g of micron-sized SiO_2–ANT display an external surface much lower than nanometric TiO_2, even in the form of aggregates.
- The isoelectric point of SiO_2 is between 1.7 and 3.5, while that of TiO_2 P25 is higher (7) [48]. In our experiments, given the pH of the suspensions (~7), it may be concluded that silica surface is negatively charged, whereas pendant amino group of $SiNH_2$–DBTP were in the form of ammonium salts, and that TiO_2 P25 was not charged.

However tentative suggestions may be put forward to explain the different reactivity between the two kinds of catalysts:

- The sensitizing materials generate exclusively singlet oxygen $^1O_2$ and possibly superoxide radical anion $O_2^{\bullet -}$. However according to the literature, the more reactive ROS, hydroxyl radical, OH• [49], was not formed under these conditions. The absence of the latter could explain the longer induction period using photosensitizing materials in comparison with TiO_2 photocatalysis. Moreover, the bacterial inactivation by $^1O_2$ requires several attacks of this ROS on *E. coli* surface before causing irreversible damages at the external membrane of the bacterium [31,50,51], compromising thereby its permeability and the vital functions taking place in this bacterial region.
- The existence of a possible defense mechanism of *E. coli* against $^1O_2$ is known. The presence in some microorganisms of carotenoid molecules contributes to trap and cancel the effect of singlet oxygen on vital tissues. In their studies on the inactivation of Gram+ and Gram− bacteria by $^1O_2$, Dahl et al. [50] noticed a better resistance of strains synthesizing carotenoids and that strains containing cyclic carotenoids were better protected than those containing acyclic molecules. Lycopene appeared as the most effective among cyclic carotenoids, followed by the zeaxanthin and finally β-carotene. These compounds are generally concentrated in the bacterial membrane (particularly in bacterial phospholipids) being an ideal location to defend the microorganisms since the first target of ROS is the bacteria membrane.

4. Conclusion

The possible use of photosensitizers supported on silica to disinfect water containing a model microorganism, *Escherichia coli*, was investigated. The photosensitizing materials were obtained by grafting various Aromatic Photosensitizers (APS) onto commercial silica powders or beads.

Depending on the structure of the APS, on the link between APS and silica, different materials were obtained and characterized by porosimetry and DRUV spectroscopy. Among the investigated photosensitizing materials, two of them showed a noticeable efficiency under irradiation at λ > 340 nm. The most efficient photosensitizers were 9,10-anthraquinone 2-carboxylic acid (ANT) and, to a lesser extent, 9,14-dicyanobenzo[b]triphenylene-3-carboxylic acid (DBTP-COOH), recently developed and patented. A slower bacterial inactivation was also observed in the presence of pure silica under irradiation. Our results indicate that the mode of introduction of the APS in silica and the amount of silica in the suspension are crucial parameters: the best efficiency was observed with powders or beads where APS was post-grafted and thus located close to the pore surface. This synthesis method also allows achieving the highest APS concentration in the materials. Contrary to TiO_2, no screening effect was observed with silica materials when increasing the amount of catalyst.

Compared with the results obtained with TiO_2, the photosensitizing materials were characterized by a longer induction period. These supported photosensitizers are known to generate Reactive Oxygen Species (ROS) such as the superoxide radical anion, $O_2^{\bullet -}$, and mainly singlet oxygen ($^1O_2$). However no hydroxyl radical, OH•, may be formed contrary to the mechanisms involved with TiO_2 photocatalysis. Our results show that $^1O_2$ and possibly $O_2^{\bullet -}$ were responsible for bacterial inactivation in aqueous suspension. In our case, the longer induction period could be attributed to the absence

of the most powerful ROS, $OH^{\bullet}$, and to an efficient bacterial defence mechanism against singlet oxygen.

To summarize, the disinfection efficiency of silica-based photosensitizing materials in aqueous suspension was demonstrated under irradiation at $\lambda > 340$ nm. This activity could open a way to a disinfecting process using only air and solar light. Higher efficiency in the visible range could be achieved by using sensitizers with spectra presenting higher molar absorption coefficient at higher wavelengths and using suitable light sources. Such materials could also be able to react with some of the organic compounds generated during the cell lysis via a photosensitizing process.

Complementary studies out of the scope of the present paper, aimed at the influence of various silica parameters (particle size and morphology, specific surface area, pendant amino functions, scattering properties in suspension) could help better understanding this inactivation mechanism.

The mode of preparation of the photosensitizing materials (grafting process) makes them very stable in aqueous suspension, without any leaking of the sensitizing aromatic molecule in water. Moreover the high efficiency of the anthraquinone-based material appears to open widespread applications, as this compound is already very often used in various industrial processes.

Appendix A. Supplementary data

Supplementary data associated with this article can be found, in the online version, at doi:10.1016/j.jphotochem.2011.01.023.

References

[1] I. Najm, R.R. Trussel, New and Emerging Drinking Water Treatment Technologies in Identifying Future Drinking Water Contaminants, National Academy Press, Washington, DC, 1999, pp. 220–243.
[2] F. Manjón, L. Villén, D. García-Fresnadillo, G. Orellana, Environ. Sci. Technol. 42 (2008) 301–307.
[3] L. Villén, F. Manjon, D. Garcıa-Fresnadillo, G. Orellana, Appl. Catal. B: Environ. 69 (2006) 1–9.
[4] P.M. Oates, P. Shanahan, M.F. Polz, Water Res. 37 (2003) 47–54.
[5] J. Hoigné, in: J. Hubrec (Ed.), The Handbook of Environmental Chemistry: Quality and Treatment of Drinking Water, Springer, Berlin, 1998.
[6] M.R. Hoffmann, S.T. Martin, W.Y. Choi, D.W. Bahnemann, Chem. Rev. 95 (1995) 69–96.
[7] D.F. Ollis, E. Pelizzetti, N. Serpone, Environ. Sci. Technol. 25 (1991) 1522–1529.
[8] Y. Kikuchi, K. Sunada, T. Iyoda, K. Hashimoto, A. Fujishima, J. Photochem. Photobiol. A: Chem. 106 (1997) 51–56.
[9] D.D. Sun, J.H. Tay, K.M. Tan, Water Res. 37 (2003) 3452–3454.
[10] A.-G. Rincon, C. Pulgarin, Appl. Catal. B: Environ. 51 (2004) 283–302.
[11] A.K. Benabbou, Z. Derriche, C. Felix, P. Lejeune, C. Guillard, Appl. Catal. B: Environ. 76 (2007) 257–263.
[12] S.A.G. Lambrechts, M.C.G. Aalders, F.D. Verbraak, J.W.M. Lagerberg, J.B. Dankert, J.J. Schuitmaker, J. Photochem. Photobiol. B: Biol. 79 (2005) 51–57.
[13] M.R Hamblin, T. Hasan, Photochem. Photobiol. Sci. 3 (2004) 436–450.
[14] M. Wainwright, J. Antimicrob. Chemother. 42 (1998) 13–28.
[15] T.A. Dahl, Photochem. Photobiol. 57 (1993) 248–254.
[16] T. Nagano, T. Tanaka, H. Mizuki, M. Hirobe, Chem. Pharm. Bull. 42 (1994) 883–887.
[17] E. Ben-Hur, N.E. Geacintov, B. Studamire, M.E. Kenney, B. Horowitz, Photochem. Photobiol. 61 (1995) 190–195.
[18] M. Shimizu-Takahama, T. Egashira, U. Takahama, Photochem. Photobiol. 33 (1981) 689–694.
[19] M. Soncin, C. Fabris, A. Busetti, D. Dei, D. Nistri, G. Roncucci, G. Jori, Photochem. Photobiol. Sci. 1 (2002) 815–819.
[20] R. Bonnett, M.A. Krysteva, I.G. Lalov, S.V. Artarsky, Water Res. 40 (2006) 1269–1275.
[21] T.G.M. Smijs, H.J. Schuitmaker, J. Photochem. Photobiol. 77 (2003) 556–560.
[22] S.A.G. Lambrechts, M.C.G. Aalders, D.H. Langeveld-Klerks, Y. Khayali, J.W.M. Lagerberg, J. Photochem. Photobiol. 79 (2004) 297–302.
[23] M. Merchat, J.D. Spikes, G. Bertoloni, G. Jori, J. Photochem. Photobiol. 35 (1996) 149–157.
[24] Z. Jackson, S. Meghji, A. MacRobert, B. Henderson, M. Wilson, Lasers Med. Sci. 14 (1999) 150–157.
[25] M.N. Usacheva, M.C. Teichert, M.A. Biel, Lasers Surg. Med. 29 (2001) 165–173.
[26] N. Komerik, M. Wilson, J. Appl. Microbiol. 92 (2002) 618–623.
[27] D. Bahnemann, in: P. Boule (Ed.), The Handbook of Environmental Chemistry, vol. 2, Springer, Berlin, Heidelberg, 1999, p. 285.
[28] M. Jemli, Z. Alouini, S. Sabbani, M. Gueddari, J. Environ. Monit. 4 (2002) 511–516.
[29] A.J. Acher, B.J. Juven, Appl. Environ. Microbiol. 33 (1977) 1019–1022.
[30] A. Acher, E. Fischer, R. Turnheim, Y. Manor, Water Res. 31 (1997) 1398–1404.
[31] M. Schafer, C. Schmitz, R. Facius, G. Horneck, B. Milow, K.H. Funken, J. Ortner, J. Photochem. Photobiol. 71 (2000) 514–523.
[32] A.T. Cooper, D.Y. Goswami, J. Sol. Energy Eng. 124 (2002) 305–310.
[33] S. Lacombe, J.Ph. Soumillion, A. El Kadib, T. Pigot, S. Blanc, R. Brown, E. Oliveros, C. Cantau, P. Saint-Cricq, Langmuir 25 (2009) 11168–11179.
[34] S. Lacombe, T. Pigot, C. Cantau, A. ElKadib, J. Ph. Soumillion, France (2009-08-28) FR2927904.(A1).
[35] V. Latour, T. Pigot, H. Cardy, M. Simon, S. Lacombe, Photochem. Photobiol. Sci. 4 (2005) 221–229.
[36] C. Cantau, S. Larribau, T. Pigot, M. Simon, M.T. Maurette, S. Lacombe, Catal. Today 122 (2007) 27–38.
[37] C. Prigent-Combaret, E. Brombacher, O. Vidal, A. Ambert, P. Lejeune, P. Landini, C. Dorel, J. Bacteriol. 183 (2001) 7213–7223.
[38] O. Vidal, R. Longin, C. Prigent-Combaret, C. Dorel, M. Hoorman, P. Lejeune, J. Bacteriol. 180 (1998) 2442–2449.
[39] J.H. Miller, A Short Course in Bacterial Genetics: A Laboratory Manual for *Escherichia coli* and Related Bacteria, Cold Spring Harbour Laboratory, Cold spring Harbor, NY, 1972, p. 352.
[40] S. Malato, P. Fernandez-Ibanez, M.I. Maldonado, J. Blanco, W. Gernjak, Catal. Today 147 (2009) 1–59.
[41] Z. Tao, M.P. Morrow, T. Asefa, K.K. Sharma, C. Duncan, A. Anan, H.S. Penefsky, J. Goodisman, A.-K. Souid, Nano Lett. 8 (2008) 1517–1526.
[42] A.J. Di Pasqua, K.K. Sharma, Y.-L. Shi, B.B. Toms, W. Ouellette, J.C. Dabrowiak, T. Asefa, J. Inorg. Biochem. 102 (2008) 1416–1423.
[43] T.-H. Bui, C. Felix, S. Pigeot-Rémy, J.-M. Herrmann, P. Lejeune, C. Guillard, J. Adv. Oxid. Technol. 11 (3) (2008) 510–518.
[44] C. Guillard, T.-H. Bui, C. Felix, V. Moules, B. Lina, P. Lejeune, C.R. Chim. 11 (2008) 107–113.
[45] C. Cantau, T. Pigot, N. Manoj, E. Oliveros, S. Lacombe, ChemPhysChem 8 (2007) 2344–2353.
[46] D.T. Sawyer, The chemistry and activation of dioxygen species in biology, in: A.E. Martell, Sawyer (Eds.), Oxygen Complexes and Oxygen Activation by Transition Metals, Plenum Press, New York, 1987, pp. 131–148.
[47] T.A. Dahl, in: G.R. Melz, R.G. Zepp, D.G. Crosby (Eds.), Aquatic and Surface Photochemistry, CRC Press, Boca Raton, 1994, p. 241.
[48] D. Gumy, C. Morais, P. Bowen, C. Pulgarin, S. Giraldo, R. Hajdu, J. Kiwi, Appl. Catal. B: Environ. 63 (2006) 76–84.
[49] M. Cho, H. Chung, W. Choi, J. Yoon, Water Res. 38 (2004) 1069.
[50] T.A. Dahl, W.R. Midden, P.E. Hartman, J. Bacteriol. 171 (1989) 2188–2194.
[51] Q. Lin, T. Tsuchido, M. Makano, Appl. Microbiol. Biotechnol. 35 (1991) 585–590.